ELSEVIER

Materials Science and Engineering A 445–446 (2007) 625–631

MATERIALS SCIENCE & ENGINEERING A

www.elsevier.com/locate/msea

Thermal desorption spectroscopy (TDS)—Application in quantitative study of hydrogen evolution and trapping in crystalline and non-crystalline materials

E. Tal-Gutelmacher, D. Eliezer*, E. Abramov

Department of Materials Engineering, Ben-Gurion University of the Negev, Beer-Sheva 84105, Israel

Received 21 May 2006; received in revised form 15 August 2006; accepted 29 September 2006

Abstract

Thermal desorption spectroscopy is a very sensitive and accurate technique for studying hydrogen's diffusion and trapping processes in crystalline and non-crystalline materials. The technique involves accurate measurement of the desorption rate of gas atoms, soluted or trapped in the material, while heating the sample at a known rate. This paper reviews the thermal desorption spectroscopy (TDS) applications in quantitative studies of hydrogen trapping and release behavior in different crystalline and non-crystalline materials. It begins with a brief overview of the physical nature of hydrogen trapping and continues with a discussion on the origins of interactions between a hydrogen atom and a trap site. Based on the simple analytical model of Lee and Lee, some examples of the assessment of comprehensive properties of hydrogen evolution and trapping in different crystalline and non-crystalline materials by means of TDS are shown and discussed in detail.

Keywords: Thermal desorption; Hydrogen; Hydrogen desorption; Hydrogen absorption

1. Introduction

Hydrogen-assisted cracking (HAC) is defined as the hydrogen-induced reduction of the fracture toughness of a metallic alloy or steel, is often manifested by delayed failure of the material and can even occur under circumstances where the fracture surface shows no evidence of brittleness [1]. HAC is induced by a critical combination of sensitive material and hydrogen content absorbed within the material. Generally, the absorbed hydrogen is not homogeneously distributed inside the material. It can be found either in the host lattice, or segregated to atomic and microstructural imperfections, such as vacancies, solute atoms, dislocations, grain boundaries, voids and second phase particles. In these localized regions, the mean residence time of a hydrogen atom is considerably longer than in a normal interstitial lattice site. In the extreme case, these regions act as sinks which retain the hydrogen atom even during thermo-mechanical loading. The generic term for this phenomenon is hydrogen trapping and these localized regions are designated as hydrogen trap sites [2,3]. Quantification of the hydrogen concentration in the material and assessment of trap sites interactions with hydrogen atoms are important in determining the likelihood of cracking.

Hydrogen probes and barnacle cells are used commonly in service, and essentially measure the "quasi-steady" permeation flux from which the distribution of the lattice hydrogen content can be deduced, albeit with some uncertainty if charging is not uniform. The hydrogen content in lattice and reversible traps can be measured, in principle, from degassing of the pre-charged material under mercury at room temperature, although confined to systems with reasonably high diffusivity, such as low-alloy carbon steels. Total hydrogen analyses by desorption at sufficiently elevated temperatures gives a measure of the hydrogen content trapped in the metal in all types of sites including irreversible trap sites. None of these methods gives information on the binding energy of the trap sites [4].

Permeation methods have also been used to determine hydrogen solubility and diffusivity in metals [5,6]. All permeation techniques involve the measurement of the time necessary for hydrogen to enter into the metal, migrate through the thickness of the specimen and then be detected on the output side. Most permeation techniques are performed with electrochemical methods [7,8], as in the pioneering work of Devanathan

* Corresponding author. Fax: +972 8 6472931.
E-mail address: deliezer@bgumail.bgu.ac.il (D. Eliezer).

0921-5093/$ – see front matter © 2006 Elsevier B.V. All rights reserved.
doi:10.1016/j.msea.2006.09.089

and Stachursky [9], where hydrogen introduction into the metal was done in an aqueous solution by, either galvanostatic or potentiostatic electrochemical charging. By means of the electrochemical hydrogen permeation method, the hydrogen content of the metal, the density of the trap sites, as well as the binding energy of the dominant reversible trap site can be measured. However, even though repeated permeation transients allows the distinction of irreversible and reversible traps, further resolution of the different types of reversible traps is usually not feasible without specific metallurgical treatment [4].

The thermal desorption method, involving measurements of hydrogen desorption flux under controlled temperature ramping conditions, is more beneficial since it can provide all the information derived from the various methods described above, including the density and binding energies of a series of trap sites, from one measurement. Furthermore, this technique is advantageous when applied to metals with a small diffusion coefficient for hydrogen atoms, e.g. Ni-based alloys, for which the test duration with other techniques may be long [4].

This paper reviews the thermal desorption spectroscopy (TDS) applications in quantitative studies of hydrogen trapping and release behavior in different crystalline and non-crystalline materials. In the beginning (Sections 2 and 3) the physical nature of hydrogen trapping and the interactions between a hydrogen atom and a trap site are briefly reviewed. The theoretical overview is followed by our experimental examples of TDS applications on crystalline and non-crystalline materials. Comprehensive properties of hydrogen evolution and trapping in the studied materials were accomplished using the simple analytical model of Lee and Lee [10–12]. As representatives of crystalline alloys, the paper addresses to our recent TDS results obtained from the study of hydrogen evolution from Ti-based alloys, whereas representative of non-crystalline alloys, our previously reported studies on hydrogen desorption from Zr-based amorphous and quasi-crystalline alloys are summarized and discussed in detail.

2. Physical nature of hydrogen trapping

The strength of a trap site, i.e. the fraction of time a hydrogen atom resides in that trap site, depends on the binding energy (E_B) of the hydrogen atom to the trap. To qualitatively describe the strength of a trap, a single hydrogen–trap interaction may be written as a first order reaction, $[H] + T = H_T$, where [H] is the diffusible hydrogen concentration, T the trap site and H_T is the trapped hydrogen concentration. The energy associated with the reaction is the hydrogen–trap binding energy (E_B). Hydrogen atoms may then be considered as either released from or captured by the trap site until equilibrium is reached. The kinetics of hydrogen trapping has been derived by McNabb and Foster [13]; $\partial\phi/\partial t = kc_L(1-\phi) - \rho\phi$, where ϕ is the fraction of traps occupied at time t, c_L the diffusible hydrogen concentration, and k and ρ are the rate constants for capture and release of hydrogen, respectively. The ratio k/ρ is proportional to $\exp(E_B/RT)$ [5]. The significance of McNabb and Foster parameters k and ρ have been discussed in depth by several authors [14,15]. The release rate constant, ρ, is interpreted [16] to be related to the trap binding energy, $\rho \approx \upsilon_T \varphi(Z) \exp[-(E_B + E_S)/RT]$, neglecting the entropy factor which is the order of unity. E_s is the saddle point energy, or the activation energy for the hydrogen atom's jump from trap sites to lattice sites, and υ_T is the vibration frequency of the trapped hydrogen atom. The function $\varphi(Z)$is given by $\varphi(Z) = (1 - e^{-z})/Z$, where $z = h\upsilon_T/k_T$ and h is Planck's constant.

Oriani [14], by applying the bimolecular theory of Waite [17], assumed a model in which each trap can hold only one hydrogen atom, which is trapped when diffusing into a small volume within a distance r_0 of an empty trap site. He interpreted the relationship between k and ρ as $k/\rho = 4\pi r_0 \lambda_2 \exp(E_B/kT)$, assuming that the vibration frequency of hydrogen at a lattice site, υ_L is the same as that at a trap site, υ_T; $\upsilon_L \approx \upsilon_T = \sqrt{E_L/2m\lambda^2} \approx 10^{13}\,s^{-1}$, where m is the mass of hydrogen and λ is the diffusive jump distance. Estimations of k and ρ values from experimental data are limited. Pressouyre and Bernstein [18] reported the value of k to be of the order of 10^{-24} to $10^{-23}\,cm^3/s$.

Abramov and co-workers [19,20] used a model accounting for diffusion and trapping based on McNabb and Foster's work [13] and Oriani's extension [14] for local equilibrium between lattice and trap sites. Fick's diffusion equation was solved for deuterium implanted on nickel. The initial concentration of trap sites and hydrogen was not uniform and was calculated by computer simulations. Trapping was accounted for at the end of each time-step in solving the diffusion equation by calculating the equilibrium between lattice and trap sites. Discrete trap energies were used but the fits were not good and it was postulated that there was a distribution of trap energies around the deuterium bubbles in the material.

In a comprehensive review on modeling of hydrogen desorption by Turnbull et al. [4], the models were divided into those considering diffusion's contribution to the overall desorption process, and those which neglect it. This paper addresses in detail only to the simple analytic approach, developed by Lee and Lee [10–12], which is based on hydrogen evolution from trap sites only, thus neglecting the diffusion processes. The rate of hydrogen release from a trap may be described by: $dc/dt = A(1-c)\exp(-E_{aT}/RT)$, where $c = (c_k^0 - c_k)/c_k^0$, c_k^0 is the amount of hydrogen in the k trapping site at time $t = 0$, c_k the amount of hydrogen in the k trapping site at time $t > 0$, A a reaction rate constant, R the gas constant, T the absolute temperature and E_{aT} is the activation energy for hydrogen release from the trapping site. This equation represents a first-order desorption, i.e. second-order desorption phenomena such as molecular desorption accompanied by recombination of adsorbed atoms are disregarded. The term $(1-c)$ represents the hydrogen content left in the trap, while $\exp(-E_{aT}/RT)$ represents the probability for hydrogen release from the trap to a 'normal' interstitial site. When a hydrogenated sample is heated at a constant rate and the rate of hydrogen desorption is plotted versus temperature, a peak is obtained. Desorption rate initially increases since the probability for hydrogen release from a trap increases faster than the decrease in the content of hydrogen in this trap. Subsequently, desorption rate decreases

to zero due to the low hydrogen content remaining in the trap. In general, the temperature producing maximal desorption is determined by the activation energy for hydrogen release from the trap, the order of desorption reaction and the heating rate. The peak intensity, on the other hand, depends on the content of trapped hydrogen and on the heating rate [21]. Qualitatively, it may be said that the temperature producing maximal desorption reflects the trapping intensity—higher temperature indicates a higher activation energy for hydrogen release. The total amount of gas atoms desorbed during heating characterizes the trap density. At the maximal hydrogen desorption, the first derivative of the equation of hydrogen's rate release equals to zero, yielding: $\varphi E_{aT}/RT_c^2 = A\ \exp[-(E_{aT}/RT_c)]$, where $T = T_0 + \varphi t$, T_0 the initial (start) temperature and T_c is the temperature at the desorption peak. This equation may be rewritten as: $\ln(\varphi/T_c^2) = \ln(AR/E_{aT}) - (E_{aT}/R)(1/T_c)$. The activation energy for hydrogen release from a trap may then be determined graphically by plotting $\ln(\varphi/T_c^2)$ versus $1/T_c$ and calculating the slope of the line. The amount of hydrogen desorbed from the material within the investigated temperature range may be obtained by integrating the plot of desorption rate versus time.

3. Various trap–hydrogen interactions

At long range relative to the atomic spacing, a hydrogen atom interacts with the defects in crystals through its elastic strain field. At short range, it interacts chemically through localized bonding with matrix atoms [22]. Due to the difficulty in making a distinction among the various chemical interactions, the local interactions are described phenomenologically in terms of a binding energy to the defect, and usually only one trap energy level is assigned to the defect.

If the binding energy, E_B is small, the corresponding traps are referred to as reversible traps and can act as either hydrogen sinks, which capture the hydrogen atoms from weaker traps, or as hydrogen sources, which deposit hydrogen atoms to stronger traps. On the other hand, large E_B give rise to irreversible traps, which normally, will not release hydrogen. The binding energy of 60 kJ/mol H for an edge dislocation or a grain boundary, is generally regarded as the upper limiting value for a reversible trap [2].

4. Examples of TDS quantitative applications on crystalline and non-crystalline materials

This chapter portrays the assessment of comprehensive properties of hydrogen evolution and trapping in different crystalline and non-crystalline materials by means of TDS. Characteristics of hydrogen desorption are evaluated based on the simple analytical model of Lee and Lee [10–12]. As representatives of crystalline alloys, we present our recent TDS results obtained from the study of hydrogen evolution from Ti-based alloys, whereas representative of non-crystalline alloys, our previously reported studies on hydrogen desorption from Zr-based amorphous and quasi-crystalline alloys are summarized and discussed in detail.

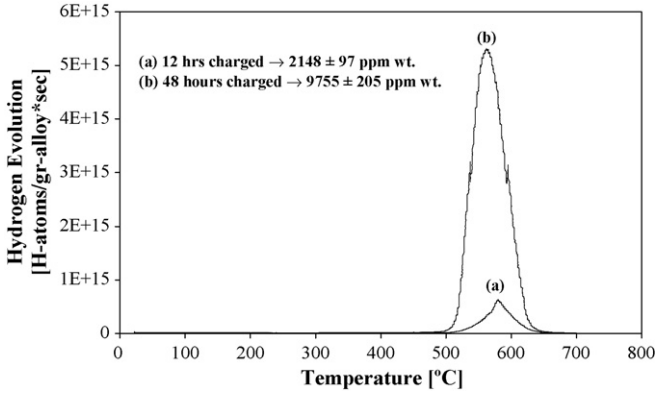

Fig. 1. TDS plots of 12 and 48 h hydrogenated Ti–6Al–4V specimens, using a constant heating rate of 5 °C/min.

4.1. Ti-based alloys

The material used for this study was a duplex-annealed Ti–6Al–4V alloy, with a bi-modal α + β microstructure, in which, 60 vol.% consists of equiaxed primary α, and 40 vol.% transformed-β (acicular secondary α), as described in detail elsewhere [23]. Hydrogen was introduced to the alloy either electrochemically, by means of cathodic charging at room temperature, in a H_3PO_4:glycerine (1:2, v/v) electrolyte, using a constant current density of 50 mA/cm^2, for different charging times, or by gaseous phase hydrogenation, conducted at 5 atm, 500 °C, for 10 h. TDS was used to determine hydrogen's evolution characteristics, and the results are supported also by other experimental techniques, i.e. hydrogen content measurements, X-ray diffraction and microscopic microstructural investigations.

4.1.1. Electrochemically charged Ti–6Al–4V

Typical TDS spectra for 12 and 48 h electrochemically charged specimens are shown in Fig. 1. The heating rate (temperature ramp) was kept constant at 5 °C/min.

Quantification of several desorption parameters is provided in Table 1.

When comparing between the TDA spectra, both plots are characterized by one main desorption peak between 562 and 580 °C. The intensity of desorption peaks increases when the sample is precharged with a higher content of hydrogen. Consequently, the total amount of hydrogen desorbed from the sample within that temperature range (i.e. the integral of desorption rate on time) increases, too. The apparent activation energy for hydrogen evolution was estimated from the shift of peaks temperatures with the increase in the applied heating rate. The typical heating rate dependence of thermal desorption from 48 h cathodically charged specimens is described in Fig. 2 and Table 2. It can be noticed that with an increased heating rate, desorption peaks are shifted to higher temperatures. The activation energy for hydrogen release was calculated from the slope of $\ln(\varphi/T_p^2)$ versus $1/T_p$, where φ is the heating rate and T_p is the peak temperature value, and it was found to be approximately 108 kJ/mol. This is a relatively high value, characteristic of irreversible trapping.

Table 1
TDS calculated parameters for 12 and 48 h electrochemically hydrogenated ($1H_3PO_4$:2glycerine, 50 mA/cm^2) Ti–6Al–4V alloy, at a constant heating rate of 5 °C/min

Charging time (h)	Temperature at desorption peak (°C)	Half height peak width (°C)	Maximal desorption rate ($\times 10^{15}$ H-atoms/g alloy s)
12	580	40.3	6.32×10^{-1}
48	562	62.5	5.32

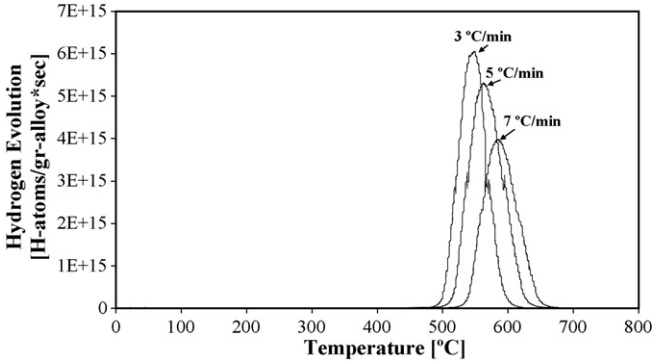

Fig. 2. TDS spectra of 48 h electrochemically hydrogenated Ti–6Al–4V alloy, at heating rates of 3 and 5 °C/min.

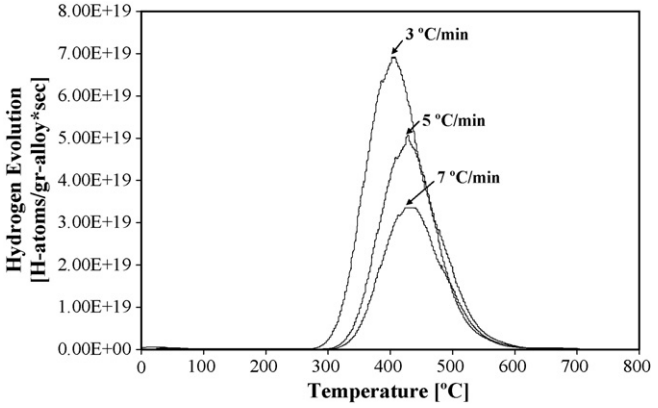

Fig. 3. TDS spectra of gas-phase charged (500 °C, 5 atm, 10 h) of Ti–6Al–4V alloy, at heating rates of 3 and 5 °C/min.

Supported by XRD data of the hydrogenated specimen before and after TDS, hydrogen evolution might occur due to titanium hydride precipitation and their dissociation at elevated temperatures. A similar value (106 kJ/mol) of the activation energy for δ-hydride dissociation was reported by Takasaki et al. [24]. Another possible site for hydrogen accumulation, which might act as irreversible trap, could be the α–β interface, as noted by Young and Scully [25].

4.1.2. Gaseous-phase charged Ti–6Al–4V

The TDS spectra of the gaseous charged Ti–6Al–4V alloy at various heating rates are presented in Fig. 3, and the calculated parameters are presented in Table 3.

The spectra exhibit one main desorption peak, i.e. one main trapping state, at a temperature range of 404–431 °C, dependant on the heating rate. The higher the heating rate, the lower the intensity of the peak, and the lower the amount of hydrogen desorbed. Based on the peaks shift to higher temperatures with the increased temperature ramp, the activation energy for hydrogen desorption was estimated to be about 100 kJ/mol. This high value is only slightly lower than the energy obtained by TDS evaluations of cathodically charged specimens. In addition to the resemblance of the desorption energies and supported by XRD data of the hydrogenated specimen before and after TDS, also in this case, hydrogen evolution may result from hydride dissociation at elevated temperatures, similar to the observations in the case of high-fugacity hydrogen charging. The lower desorption temperature and the slightly smaller activation energy for hydrogen release, may result from the different initial microstructure before TDS. In the electrochemically charged specimens, their microstructure, in addition to the Ti-hydride, consists of also Ti-α and -β phases, whose fraction appeared to be larger than the hydride, while in the gas-phase charged specimens, the XRD revealed the sole existence of δ-TiH_2. Another apparent difference between the TDS plots of specimens charged with high- and low-fugacity hydrogen, is the desorption rate (height of the desorption peaks). As expected due to the initially appreciably higher amount of absorbed hydrogen, in the gas charged

Table 2
Summary of TDS calculated parameters of 48 h electrochemically hydrogenated Ti–6Al–4V alloy, at heating rates of 3, 5 and 7 °C/min

Heating rate (°C/min)	Temperature at desorption peak (°C)	Half height peak width (°C)	Maximal desorption rate ($\times 10^{15}$ H-atoms/g alloy s)
3	548	45	6.06
5	562	62.5	5.32
7	584	66	3.94

Table 3
Summary of TDS calculated parameters of gas-phase charged (500 °C, 5 atm, 10 h) Ti–6Al–4V alloy, at different heating rates (3, 5, 7 °C/min)

Heating rate (°C/min)	Temperature at desorption peak (°C)	Half height peak width (°C)	Maximal desorption rate ($\times 10^{15}$ H-atoms/g alloy s)
3	404	101	3.35×10^4
5	427	110	5.08×10^4
7	431	114.8	6.92×10^4

material the desorption rate is significantly higher (by four orders of magnitude) in comparison to the cathodically charged material.

4.2. Zr–Cu–Ni–Al amorphous and quasi-crystalline alloys

Amorphous and quasi-crystalline alloys have been shown to possess structural characteristics and properties markedly different from their crystalline counterparts. Since the storage capacity of hydrogen in metals and alloys is determined by the chemical interactions between the metal and the hydrogen atom, as well as by the type, size and number of potential interstitial sites, one of the many technological applications foreseen for these amorphous and quasi-crystalline materials was hydrogen storage, based on the combination of favorable chemical composition and either amorphous or icosahedral structure which is dominated by local tetrahedral order. Amorphous and quasi-crystalline Zr–Cu–Ni–Al alloys were initially reported to absorb high amounts of hydrogen [26]. However, in a previous study [27], it was revealed that hydrogen release from these alloys was inhibited by the presence of a thin oxide layer. To overcome this problem, both melt-spun amorphous and annealed quasi-crystalline ribbons were coated by vapor deposition with a thin layer of palladium, approximately 100 nm thick. This layer was found to enhance significantly the absorption/desorption behavior of hydrogen in these alloys [28,29].

Typical TDS spectra for Pd-coated amorphous and quasi-crystalline $Zr_{69.5}Cu_{12}Ni_{11}Al_{7.5}$ specimens, reported recently [30], are shown in Fig. 4(a and b), respectively. In both cases, the specimens were first charged with different deuterium concentrations, applying a constant current density, but different charging periods. The heating rate (temperature ramp) was kept constant at 5 °C/min.

As expected, the intensity of desorption peaks increased when the sample was precharged with a higher content of deuterium. Consequently, the total amount of deuterium desorbed from the sample within that temperature range (i.e. the integral of desorption rate on time) increased, too. One desorption peak was observed at 557 °C for the amorphous material pre-charged to 0.1 D/M. However, when the amorphous material was preloaded with 0.6 D/M, four peaks are evident (at 253, 402, 501 and 560 °C, respectively). Four peaks (at 225, 332, 410 and 532 °C, respectively) were also noticed for the amorphous material preloaded with 1.6 H/M. Thus, it was concluded that as the Pd-coated amorphous alloy was charged with higher concentrations of deuterium, the desorption peaks in the TDS spectra were both shifted to lower temperatures and increase in number. Since phase transformations in the Zr–Cu–Ni–Al system take place in parallel to desorption, we related the desorption peaks at higher temperatures to deuterium release during the decomposition of quasi-crystals, whose temperature decreases as deuterium content increases [30]. Comparing these TDS results to those reported on the uncoated alloy [27], the amount of deuterium desorbed from the Pd-coated amorphous alloy is higher by at least an order of magnitude, emphasizing the contribution of the Pd-coating to the improved absorption/desorption behavior of both hydrogen and deuterium in the $Zr_{69.5}Cu_{12}Ni_{11}Al_{7.5}$ amorphous alloy.

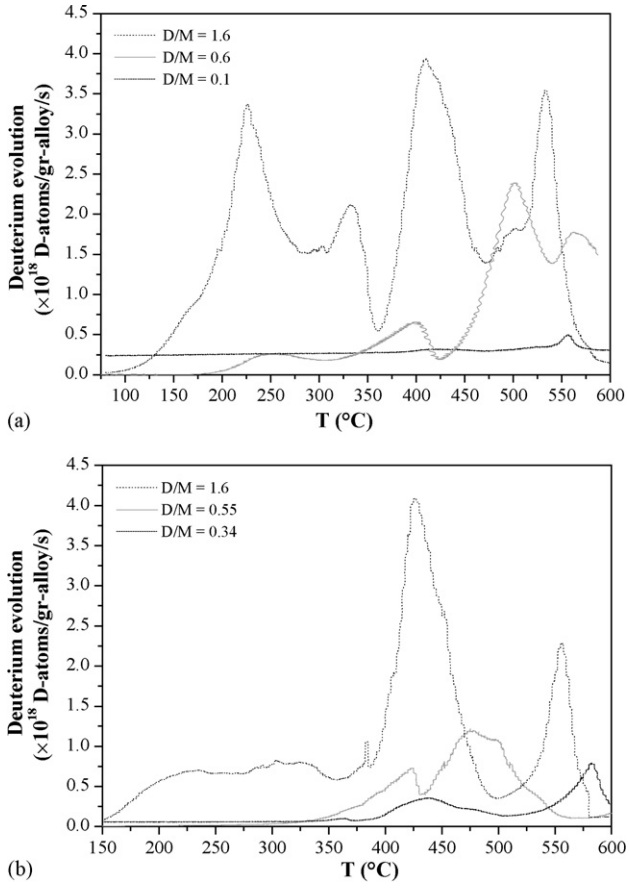

Fig. 4. The dependence of desorption profile on the initial deuterium loading for: (a) amorphous, and (b) partially quasi-crystalline Pd-coated $Zr_{69.5}Cu_{12}Ni_{11}Al_{7.5}$ alloys [30].

In the case of the partially quasi-crystalline alloy, the TDS peaks were also shifted to lower temperatures when the material was preloaded with higher concentrations of deuterium. Here, the shift was attributed to a higher tendency of deuterium atoms to occupy new trap sites of lower binding energy when more deuterium was introduced into the material. In the case of the quasi-crystalline alloy, it was not as clear that the number of desorption peaks increases with increasing deuterium loadings. All peaks appearing at temperatures higher than 470 °C may be associated also with decomposition of the quasi-crystalline phase into Zr-based crystalline phases as well as with Zr-based hydride formation [28]. Several significant differences were noticed when comparing the current TDS results for the Pd-coated quasi-crystalline alloy to those reported for the uncoated quasi-crystalline alloy [27]. The Pd coating allowed desorption to start at a much lower temperature, exposed additional desorption peaks, allowed a better differentiation between desorption spectra from samples that were charged for different periods under otherwise the same conditions, and allowed recovery of most of the deuterium that was loaded into the material. In addition, while the desorption peaks of the Pd-coated samples were shifted to lower temperatures when the material was preloaded with higher concentrations of deuterium, those of uncoated

samples were shifted to higher temperatures [27]. These differences clearly demonstrated the major role of the oxide surface barrier layer in deuterium desorption from the Zr-based quasi-crystalline alloy. Since to the best of our knowledge, hardly any studies have been reported on hydrogen trapping in quasi-crystalline alloys, we assumed that the possible trap sites in the quasi-crystalline Pd-coated $Zr_{69.5}Cu_{12}Ni_{11}Al_{7.5}$ alloy could be defects, including dislocations which are inevitably accompanied by strain fields (phason strain) [30]. This strained region may produce more free volume for trapping of small atoms such as hydrogen. Yet, the mechanisms of hydrogen trapping in quasi-crystalline materials remains to be determined.

Fig. 5(a and b) reveals the typical heating rate dependence of thermal desorption from amorphous and quasi-crystalline specimens, respectively, precharged with 1.6 D/M. It was noticed that with an increased heating rate, the desorption peaks of either amorphous or quasi-crystalline Pd-coated $Zr_{69.5}Cu_{12}Ni_{11}Al_{7.5}$ samples were shifted to higher temperatures; in addition, the total amount of desorbed hydrogen decreased [30].

Following Lee and Lee procedure, in the desorption spectra of the Pd-coated quasi-crystalline alloy, the activation energy was found to be $E_{aT} = 2.4$ and 17.7 kJ/mol for the first peak and second peak, respectively, much lower values than those reported for the uncoated quasi-crystalline alloy ($E_{aT} \sim 37.6$ kJ/mol). However, they were larger than the activation energy values for desorption from different traps in a Pd-coated amorphous alloy that was charged with an identical deuterium content of 1.6 D/M ($E_{aT} = 1.5$, 1.6, 2.7 and 5.3 kJ/mol for the first, second, third and fourth peaks, respectively) [30]. It should be noted that these results indicate that the traps in either amorphous or quasi-crystalline Zr–Cu–Ni–Al alloys are reversible, because the activation energy values are all much lower than the upper limit value of 60 kJ/mol that was suggested for an edge dislocation, grain boundary, or other reversible traps [2]. Deuterium release from the amorphous alloy started at lower temperatures in comparison to the quasi-crystalline counterpart. This behavior probably resulted from traps with higher binding energy in the quasi-crystalline structure, although it could also be influenced by phase transformations that occurred during heating [30].

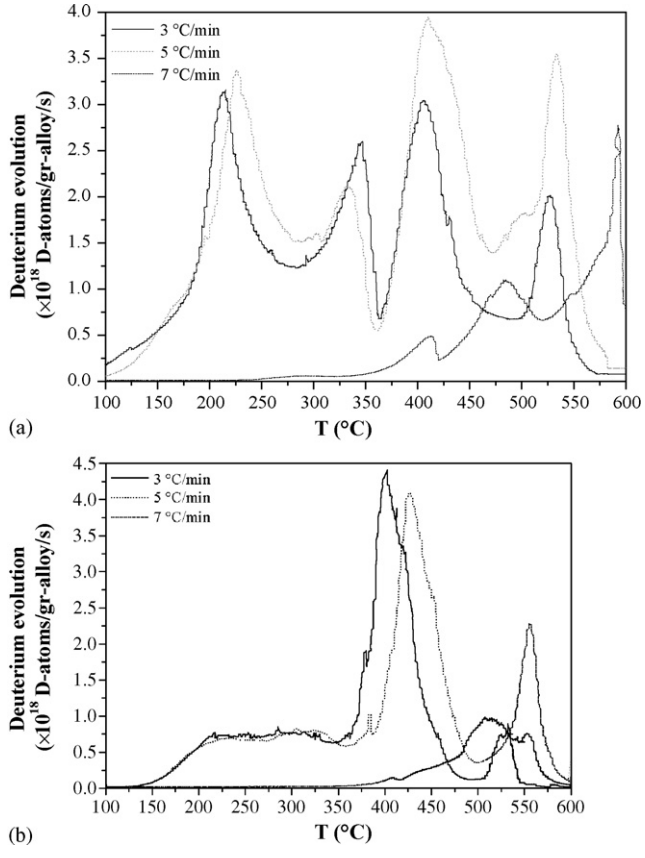

Fig. 5. Heating rate dependence of deuterium evolution from Pd-coated amorphous (a) and quasi-crystalline (b) $Zr_{69.5}Cu_{12}Ni_{11}Al_{7.5}$ alloys [30].

5. Conclusions

- The purpose of this paper was to display the powerful abilities of thermal desorption spectroscopy for studying the hydrogen's diffusion process, its absorption/desorption behavior and trapping effects in a wide variety of crystalline and non-crystalline materials.
- For demonstration, the characteristics of hydrogen evolution from either crystalline (Ti–6Al–4V alloy) or non-crystalline (Zr–Cu–Ni–Al amorphous and quasi-crystalline alloys) materials, evaluated by means of TDS, were shown.
- In crystalline Ti–6Al–4V alloy, irrespective of the way hydrogen is introduced to the alloy, the hydrogen evolution plots exhibited only one main desorption peak, at elevated temperatures, with a significantly high activation energy value for hydrogen release, attributed to titanium's hydride dissociation at elevated temperatures.
- In contrast, in quasi-crystalline and amorphous Zr–Cu–Ni–Al alloy, the hydrogen evolution was found to be a more complex process, being affected by various parameters, such as the presence of different trapping sites in either structure, the phase transformations which take place during annealing, for instance, the decomposition of either the matrix or the formation and dissociation of Zr-based hydrides.

References

[1] R.A. Oriani, Corrosion 43 (7) (1987) 390.
[2] G.M. Pressouyre, I.M. Bernstein, Metall. Trans. 12A (1981) 835.
[3] I.M. Bernstein, G.M. Pressouyre, in: R.A. Oriani, J.P. Hirth, M. Smialowski (Eds.), Hydrogen Degradation of Ferrous Alloys, Noyes Publications, Park Ridge, NJ, 1985, p. 641.
[4] A. Turnbull, R.B. Hutchings, D.H. Ferriss, Mater. Sci. Eng. A 238 (1997) 317.
[5] H.H. Johnson, Metall. Trans. 19B (1988) 691.
[6] R. Lin, H.H. Johnson, Acta Metall. 30 (1982) 1819.
[7] I.M. Bernstein, A.W. Thompson, in: N.F. Fiore, B.J. Berkowitz (Eds.), Advanced Techniques for Characterizing Hydrogen in Metals, TMS-AIME, Kentucky, 1981, p. 89.
[8] R. Kircheim, R.B. McLellan, J. Electrochem. Soc. 127 (11) (1980) 2419.
[9] M.A. Devanathan, Z.O.J. Stachursky, Proc. R. Soc. A270 (1962) 90.
[10] S.M. Lee, J.Y.L. Lee, Appl. Phys. 63 (9) (1988) 4758.
[11] W.Y. Choo, J.Y. Lee, Metall. Trans. A13 (1982) 135.
[12] J.L. Lee, J.Y. Lee, Met. Sci. 17 (1983) 426.
[13] A. McNabb, P.K. Foster, Trans. TMS-AIME 227 (1963) 618.

[14] R.A. Oriani, Proceedings of Fundamental Aspects of Stress Corrosion Cracking Conference, NACE, Houston, TX, 1967, p. 32.
[15] M. Iino, Acta Metall. 30 (1982) 367.
[16] C. Zener, in: W. Shockeley (Ed.), Imperfections in Neary Perfect Crystals, Wiley, New York, NY, 1952, p. 289.
[17] T.R. Waite, Phys. Rev. 107 (1957) 463.
[18] G.M. Pressouyre, I.M. Bernstein, Acta Metall. 27 (1979) 89.
[19] E. Abramov, D. Eliezer, Metall. Mater. Trans. A25 (1994) 949.
[20] R.G. Macaulay-Newcombe, M. Riehm, D.A. Thompson, W.W. Smeltzer, E. Abramov, Radic. Effects Def. Solids 117 (1991) 285.
[21] G. Carter, Vacuum 12 (1962) 245.
[22] J.P. Hirth, in: R.A. Oriani, J.P. Hirth, M. Smialowski (Eds.), Hydrogen Degradation of Ferrous Alloys, Noyes Publications, Park Ridge, NJ, 1985, p. 131.
[23] E. Tal-Gutelmacher, D. Eliezer, D. Eylon, Mater. Sci. Eng. A 381 (1–2) (2004) 230.
[24] A. Takasaki, Y. Furuya, K. Ojima, Y. Taneda, J. Alloys Compd. 224 (1995) 269.
[25] G.A. Young, J.R. Scully, Scripta Metall. Mater. 28 (1993) 507.
[26] U. Koester, J. Meinhardt, S. Roos, H. Liebertz, Appl. Phys. Lett. 69 (1996) 179.
[27] N. Eliaz, D. Eliezer, E. Abramov, D. Zander, U. Köster, J. Alloys Compd. 305 (1–2) (2000) 272.
[28] D. Zander, E. Tal-Gutelmacher, L. Jastrow, U. Köster, D. Eliezer, J. Alloys Compd. 356–357 (2003) 654.
[29] E. Tal-Gutelmacher, N. Eliaz, D. Eliezer, D. Zander, L. Jastrow, U. Köster, Mater. Sci. Eng. A 358 (1–2) (2003) 219.
[30] E. Tal-Gutelmacher, N. Eliaz, D. Eliezer, Scripta Mater. 52 (2005) 777.